Table of Contents

Supplementary Table S1. CellProfiler pipeline used for quantification of cell shape features.

Module	Description
GaussianFilter	To smooth nuclear staining for improved identification of individual nuclei (primary object). Sigma: 2
ImageMath	To normalize wheat germ agglutinin signal from improved segmentation of cell membrane staining (secondary object). Operation: Log transform (base 2) Multiply the first image by: 1.0 Raise the power of the result by 0.5 Multiply the result by: 1.0 Add to result: 0 Set values less then 0 equal to 0: Yes Set values greater than 1 equal to 1? Yes Ignore the image mask? No
IdentifyPrimaryObjects	To identify individual cell nuclei, stained by DAPI. Object: Nuclei Typical diameter (Min, Max): 4, 20 Discard objects outside the diameter range? Yes Discard objects touching the border of the image? Yes Threshold strategy: Adaptive Thresholding method: minimum cross entropy Threshold smoothing scale: 0 Threshold correction factor: 1.5 Lower and upper bounds on threshold: 0.0005, 1.0 Method to distinguish clumped objects: Shape Method to draw dividing lines between clumped objects: Intensity Automatically calculate size of smoothing filter for declumping? Yes Automatically calculate minimum allowed distance between local maxima? No Speed up by using lower-resolution images to find local maxima? Yes Fill holes in identified objects? After both thresholding and declumping Handling of objects if excessive number of objects identified: Continue
IdentifySecondaryObjects	To identify cytoplasmic domain, stained by wheat germ agglutinin, associated with each nuclei. Select the input objects: Nuclei Name the objects to be identified: Cells Select the method to identify the secondary objects: Watershed - image Threshold strategy: Global Thresholding Method: Minimum cross entropy Threshold smoothing scale: 1.3488 Threshold correction factor: 2.0 Lower and upper bounds on threshold: 0.075, 0.9 Fill holes in identified objects? Yes Discard secondary objects touching the border of the image? Yes Retain outlines of the identified secondary objects? Yes
MeasureObjectSizeShape	All available shape features are examined on a cell-by-cell basis.*
ExportToDatabase	Export cell shape features for further analysis as described in The Methods.

* All shape features are available with definitions in the CellProfiler manual (http://cellprofiler.org/manuals/) under MeasureObjectSizeShape. Nuclear features were similarly analyzed, and no differences were observed between different polarization states.

Processing time was approximately 2 h per plate for 1536 images on a 12-core workstation running 12 CellProfiler workers in parallel.

Supplementary Table S2. Panel of drugs included in high-content morphological screening.

Drug	Target(s)	Concentration range
GW2580	CSF1R	10 µM-100 pM
CEP32496	CSF1R	6 µM-60 pM
BLZ945	CSF1R	6 µM-60 pM
OSI930	CSF1R/CKIT	10 µM-100 pM
PLX3397	CSF1R/CKIT	10 µM-100 pM
DASATINIB	Abl/Src/CKIT	10 µM-100 pM
SUNITINIB	PDGFR/VEGFR/CKIT	10 µM-100 pM
ABT869	VEGF/PDGF/KDR/CSF1R	6 µM-60 pM
IMATINIB	Abl/CKIT/PDGFR	10 µM-100 pM
FORETINIB	HGFR/VEGFR	10 µM-100 pM
XL228	IGFR/FGFR	10 µM-100 pM
GEFITINIB	EGFR	10 µM-100 pM
PD0325901	MEK	10 µM-100 pM
TRAMETINIB	MEK	10 µM-100 pM
BENTAMAPIMOD	JNK	10 µM-100 pM
DABRAFENIB	BRAF	10 µM-100 pM
VEMURAFINIB	BRAF	10 µM-100 pM
CRIZOTINIB	ALK/ROS1	10 µM-100 pM
UNC2025	MERTK	10 µM-100 pM
INDOXIMOD	IDO	10 µM-100 pM
CELECOXIB	COX2	10 µM-100 pM
RAPAMYCIN	mTOR	10 µM-100 pM
NIK12192	V-ATPase	10 µM-100 pM
TRICHOSTATIN A	HDAC	10 µM-100 pM
IBET151	BET	10 µM-100 pM
TMP195	HDAC	10 µM-100 pM
BYL719	PI3Ka	10 µM-100 pM
GDC0941	PI3Ka/g	10 µM-100 pM
BKM120	PI3K	10 µM-100 pM
R848	TLR7/8	10 µM-100 pM
MOTOLIMOD	TLR8	10 µM-100 pM
GS9620	TLR7	10 µM-100 pM

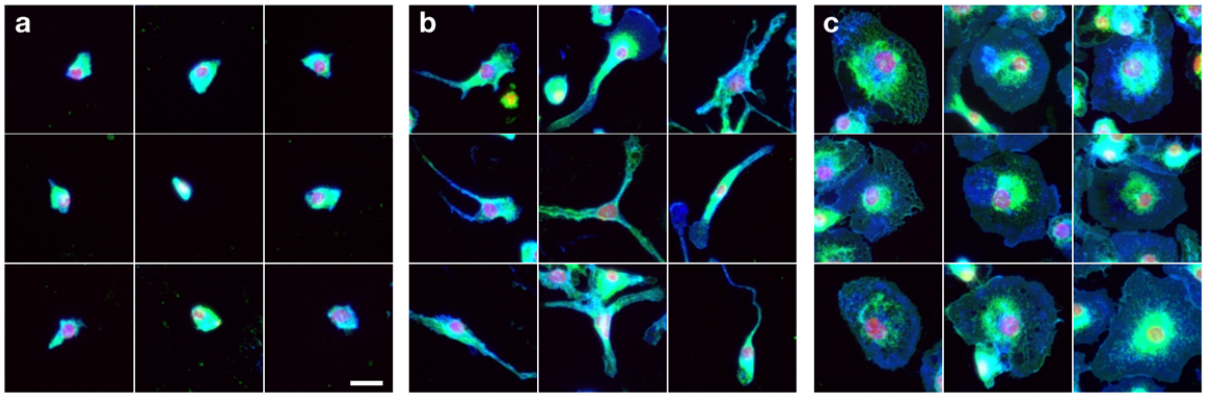

Supplementary Figure S1. Example CellProfiler training data. Examples of training data provided to CellProfiler Analyst for stratification of murine M0 (undifferentiated monocytes, **a**), M2-like (M-CSF derived, **b**), and M1-like (LPS/IFN-γ treated, **c**). Scale bar: 25 μm.

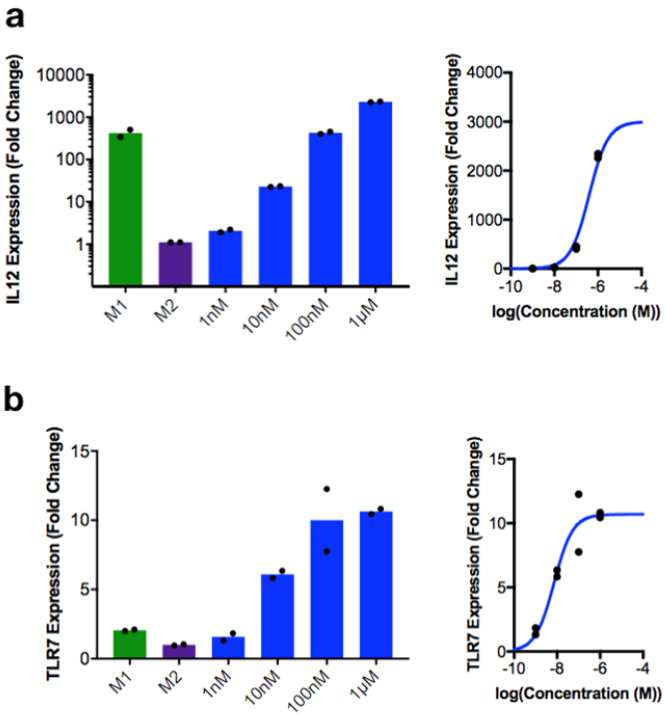

Supplementary Figure S2. IL12 and TLR7 expression in response to R848. Murine M2-like (IL-4 treated) macrophages were cultured in the presence of R848 for 24 hours. **a,** IL12 transcription indicates response to nM concentrations of R848. **b,** TLR7 expression increased in response to R848, likely sensitizing response to drug treatment. IC50 values (IL12: logIC50 = -6.40 ± 0.051; TLR7: logIC50 = -8.14 ± 0.17) are in good agreement with those obtained for M1 enrichment by high-content screening approaches (logIC50 = -7.84 ± 0.159). Expression values represent fold change relative to M2 controls; data represented the mean of two independent samples from a single experiment.

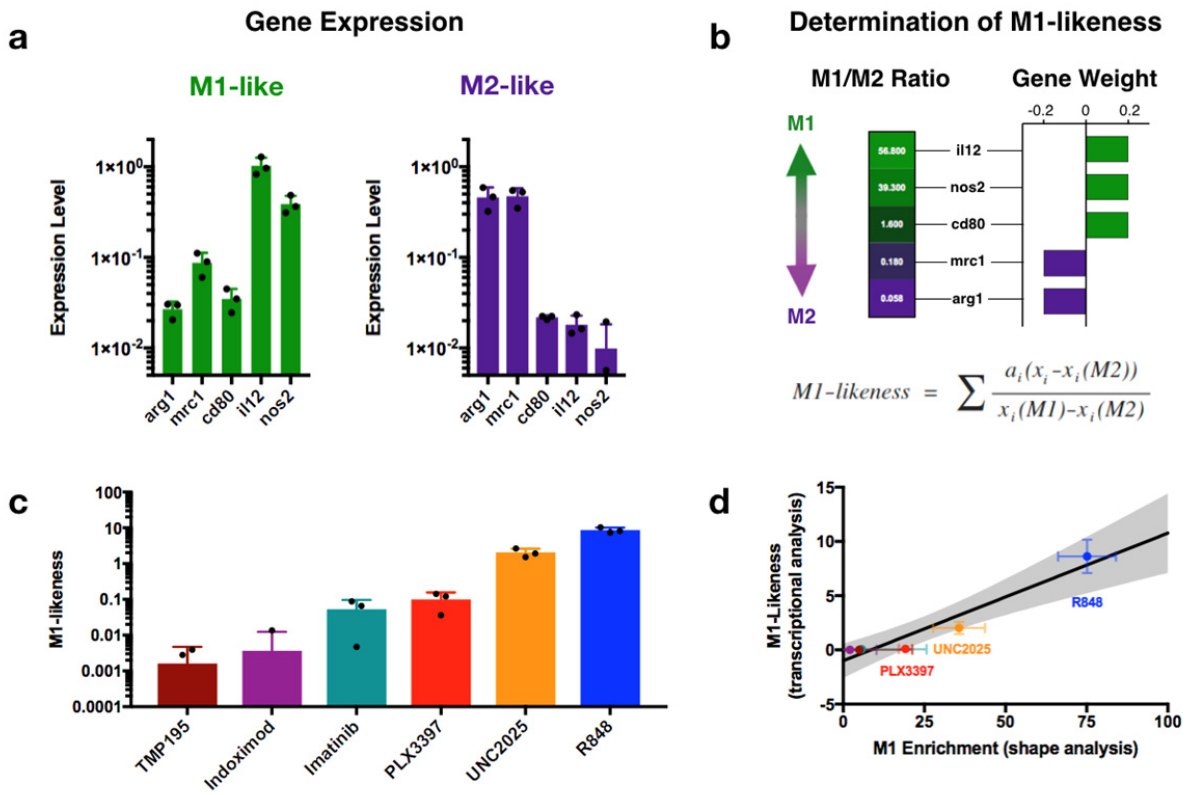

Supplementary Figure S3. Validation of high-content screening by transcriptional phenotyping. a, Gene expression of M1-like and M2-like murine macrophages, expressed as fold change relative to *hprt*; mean ± s.d., N=3 independent samples from a single experiment. **b,** Simultaneous examination of multiple statistically and biologically relevant transcriptional markers provides a robust metric of phenotype: M1-likeness. Determination of M1-likeness, accounting for both canonical M1- and M2-like gene expression levels (x_i) with assigned gene weights (a_i). M1-likeness is determined by summing the changes in expression for each gene resulting from treatment, normalized to the range of expression observed in the training data. **c,** Transcriptional M1-likeness in response to a select validation set of drugs, indicating the strong ability of R848 to induce M1-like gene transcription. Data represent mean ± s.d., N=3 independent samples from a single experiment. **d**, Correlation of morphological (mean ± range, N=2 independent samples) and transcriptional (mean ± s.d, N=3 independent samples) phenotyping scores, indicative of the ability of high-content screening (M1 enrichment) to accurately predict macrophage phenotype (M1-likeness). Black line: linear fit with 95% CI (shaded); R^2>0.92.

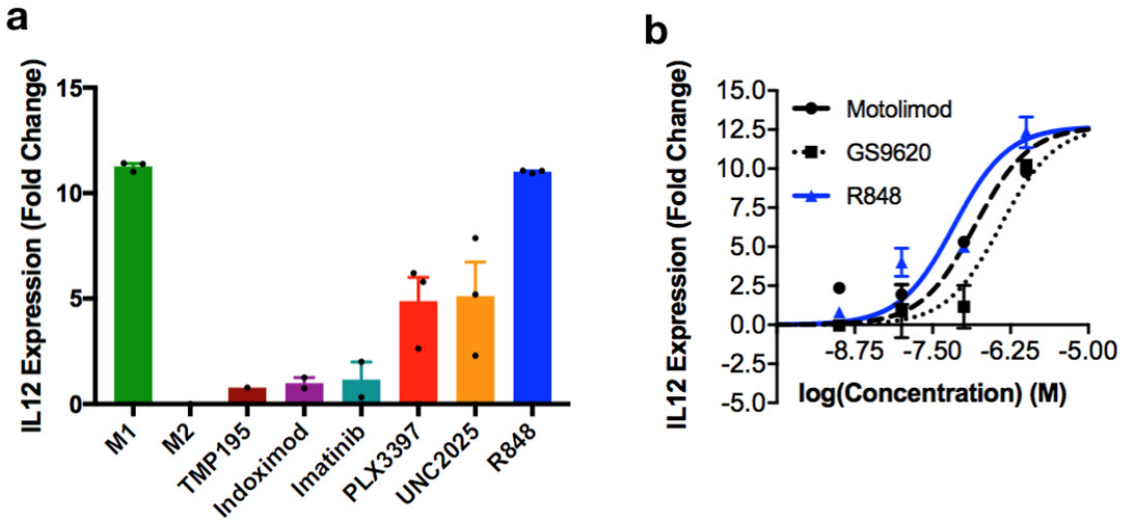

Supplementary Figure S4. Validation of drug activity by transcriptional phenotyping of human macrophages. The response of human macrophages to the drugs screened was validated in CD14+CD11b+ human monocytes derived in M-CSF, using IL12 as an indicator of M1-like polarization. Human macrophages were polarized to an M2-state (IL-4 induction, 24 hrs) prior to drug treatment in the presence of IFN-γ **a**, IL12 expression as fold change relative to M2 controls; mean ± s.d., N=3 independent samples from a single experiment. Response toward this validation set of drugs was similar to that observed in murine cells (Supplementary Figure S3). **b,** Dose response of IL12 induction in response to motolimod (TLR8), GS9620 (TLR7), and R848 (TLR7/8). Data represent mean ± s.d., N=2 independent samples from a single experiment. R848 demonstrated the greatest response in human macrophages, with an EC50 of 69.7nM.

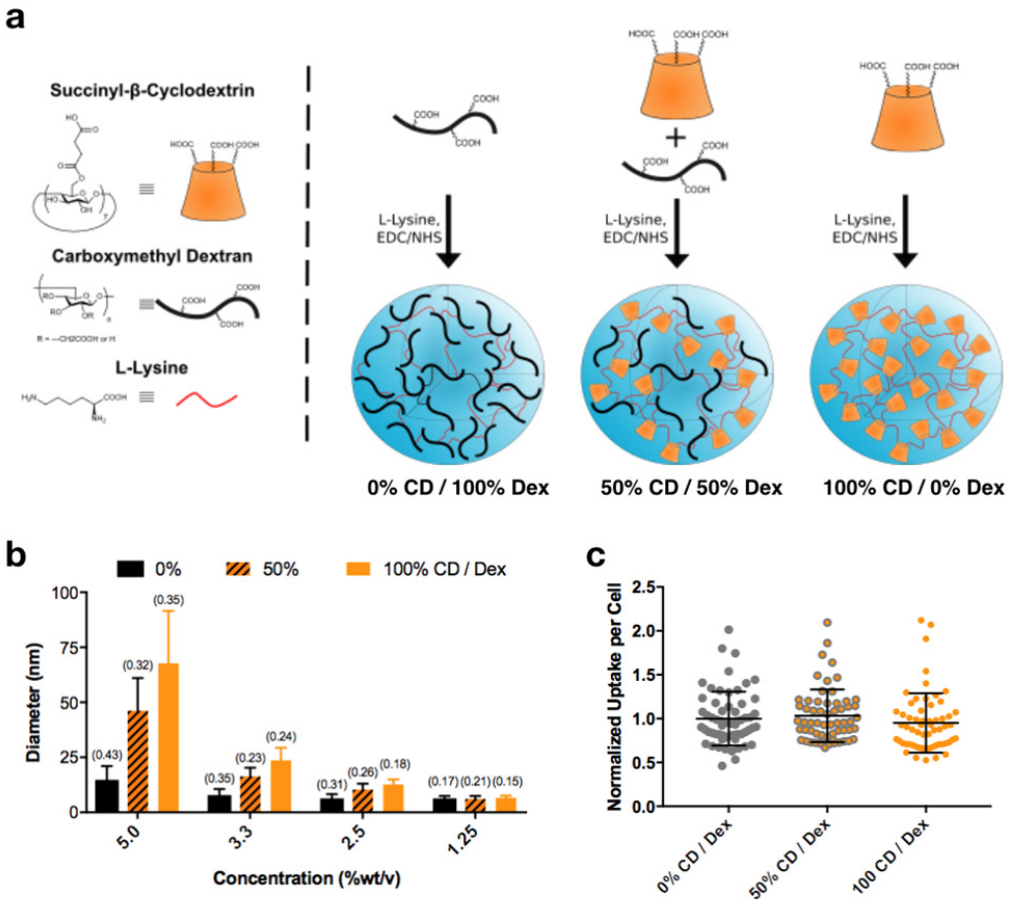

Supplementary Figure S5. Cyclodextrin content contributes to nanoparticle size but does not influence macrophage affinity. a, Nanoparticles were formed consisting of succinyl-β-cyclodextrin (CD, orange) and carboxymethyl dextran (Dex, black) at defined ratios of 0%, 50%, and 100% CD/Dex by L-Lysine crosslinking. **b**, Under equivalent crosslinking conditions, CD contributed to formation of larger nanoparticles and reduction in polydispersity. Data represent the mean ± s.d. of a single sample (N>1000 reads); polydispersity index (PDI) is indicated in parentheses. **c,** Uptake of nanoparticles by RAW 264.7 cells *in vitro* was independent of particle composition (ANOVA, P = 0.37), indicating the use of CD as a base material does not inhibit phagocytosis relative to established dextran nanoparticles [1]. Data are normalized to the 0% CD/Dex condition and represent mean ± s.d., N = 60 cells per condition from two independent repeats per condition.

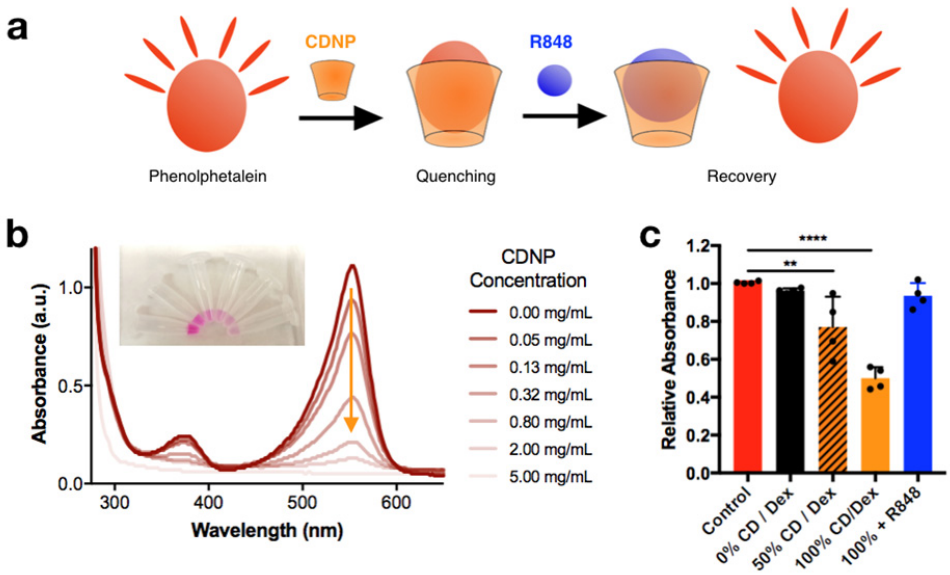

Supplementary Figure S6. Cyclodextrin content is required for specific guest-host interaction. a, The ability of CDNPs to bind small molecules was assessed by a chromatographic competitive binding assay. **b,** Phenolphthalein absorbance (550 nm) was quenched (indicated, arrow) in the presence of increasing CDNP concentrations. Data represent the average of three independent measurements. Inset: micrograph with increasing CDNP concentration from left to right. **c,** Quenching of absorbance (550 nm) in the presence of nanoparticle (0.5 mg mL^{-1}) was dependent on CD content. Addition of R848 (20 mM) competitively bound to the 100% CD/Dex particle, recovering phenolphetalein absorbance. Data are expressed as mean ± s.d.; N=4 independent samples; ***P=0.008, ****P<0.0001 (ANOVA, Tukey HSD) relative to nanoparticle free control.

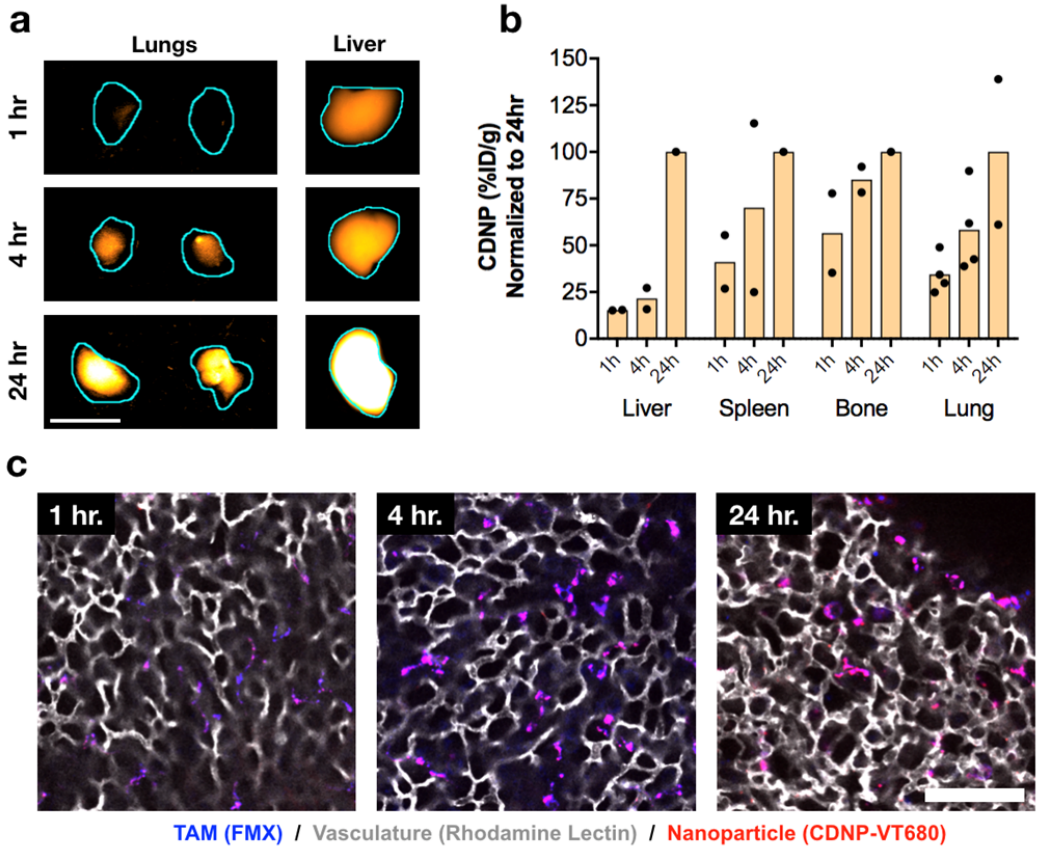

Supplementary Figure S7. Temporal biodistribution of CDNP. The biodistribution of CDNP-VT680 was examined in C57BL/6 mice at 1hr (N = 2 mice), 4hr (N = 2 mice), and 24hr (N=1 mouse). For groups performed in duplicate, images are representative of the two independent samples. **a,** Fluorescence reflectance imaging of CDNP-VT680 accumulation in lungs and liver at 1, 4, and 24 hours following administration (λ_{ex} = 620-650 nm, λ_{em} = 680-710 nm). Tissues are outlined (cyan) for clarity. Scale bar: 5.0 mm. **b,** Corresponding quantified biodistribution of CDNP-VT680 was examined in duplicate and presented following normalization to the 24 hour time point. Data are presented as the mean of N=2 mice for 1hr and 4hr, N=1 mouse for 24hr. For lung tissue, both lungs are included in analysis. **c,** Distribution of CDNP-VT680 within the lung was examined by confocal fluorescence microscopy in lung tissue following perfusion. Scale bar: 50 μm. Notably, CDNP-VT680 co-localizes with macrophage signal within the lung, does not result in vascular casts, and increases in macrophages over time.

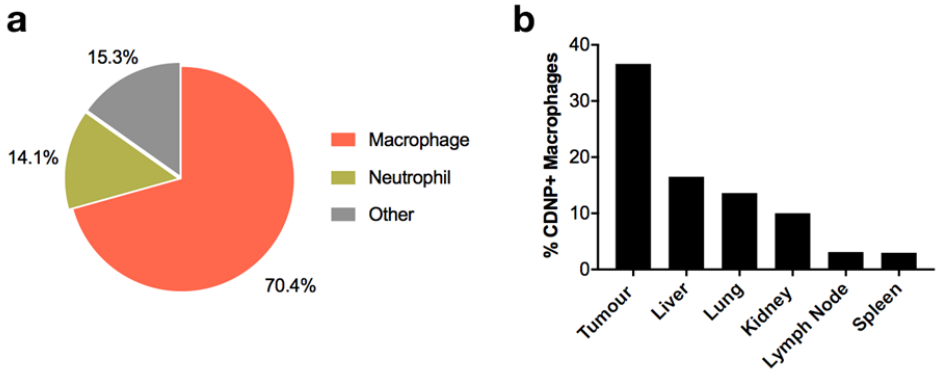

Supplementary Figure S8. CDNPs preferentially accumulate in tumour associated macrophages. At 24 hours following administration of CDNP-VT680, relevant tissues were harvested from a MerTK$^{GFP/+}$ mouse bearing an MC38-H2B-mApple tumour. **a,** Flow cytometry was performed to identify the distribution of CDNP-VT680 to immune cells in tumours, including TAM (CD45+MerTK+Ly6G-), neutrophils (CD45+MerTK-Ly6G+), and other tumour associated immune cells (CD45+). **b,** Percentage of tissue macrophages that contain high levels of CDNP-VT680 after a single i.v. administration. Notably, tumour associated macrophages have higher CDNP uptake compared to macrophages in other tissues.

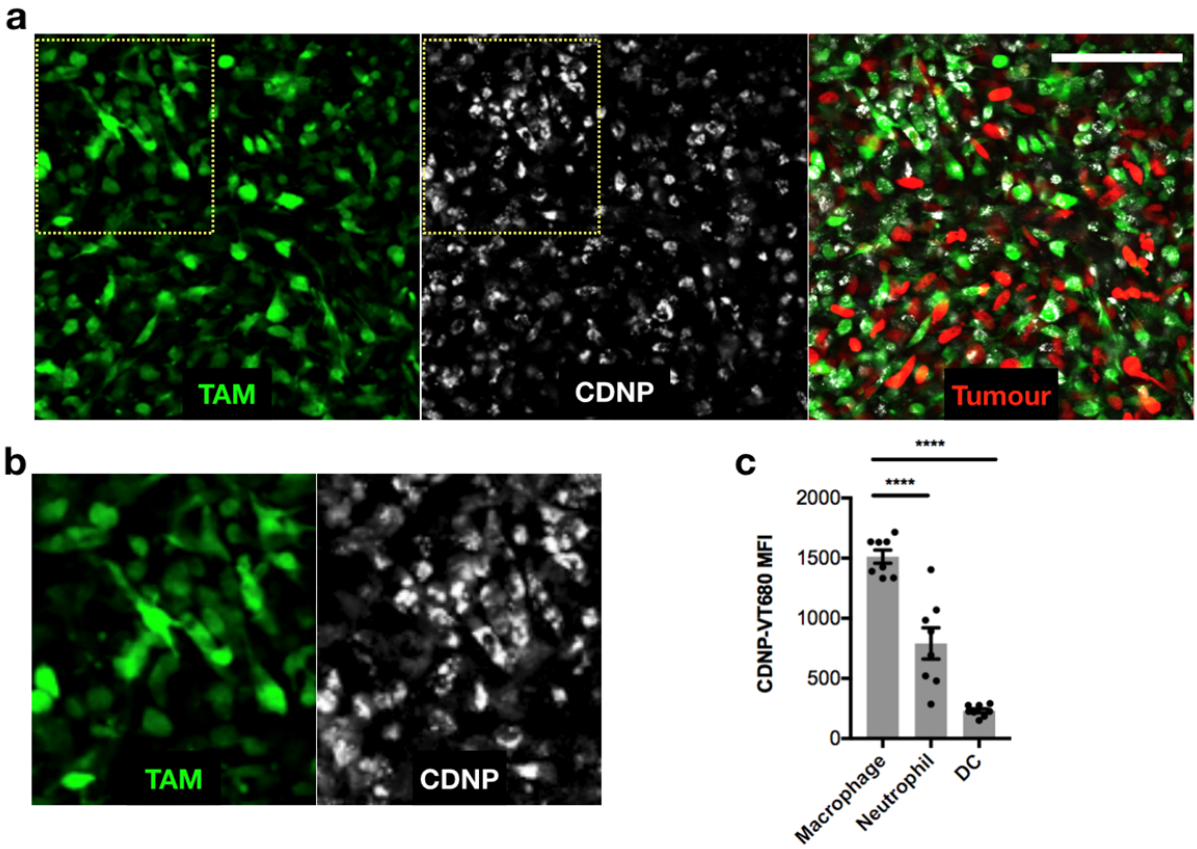

Supplementary Figure S9. CDNP cellular distribution is macrophage targeted. a, Images of tumours were acquired at 24 hours following i.v. administration of CDNP-VT680 (CDNP, gray) in MerTK$^{GPF/+}$ (TAM, green) mice bearing MC38-H2B-Apple tumours (Tumour, red). Results are representative of N=3 independent experiments. Scale bar: 100 µm. Note the near exclusive distribution of CDNP to TAMs, expanded (**b**) for clarity. **c**, Flow cytometry was performed to identify the cellular distribution of CDNP-VT680 to immune cells 24 hours after i.v. administration in C57BL/6 mice bearing MC38 in tumours, including TAMs (CD45+F4/80+), neutrophils (CD45+Ly6G+), and dendritic cells (CD45+CD11c+MHCII+F4/80-). Accumulation was highest in F4/80+ macrophages and much lower in dendritic cells. Data represent mean ± s.d.; N=8 tumours; ****P<0.0001 (ANOVA, Tukey HSD).

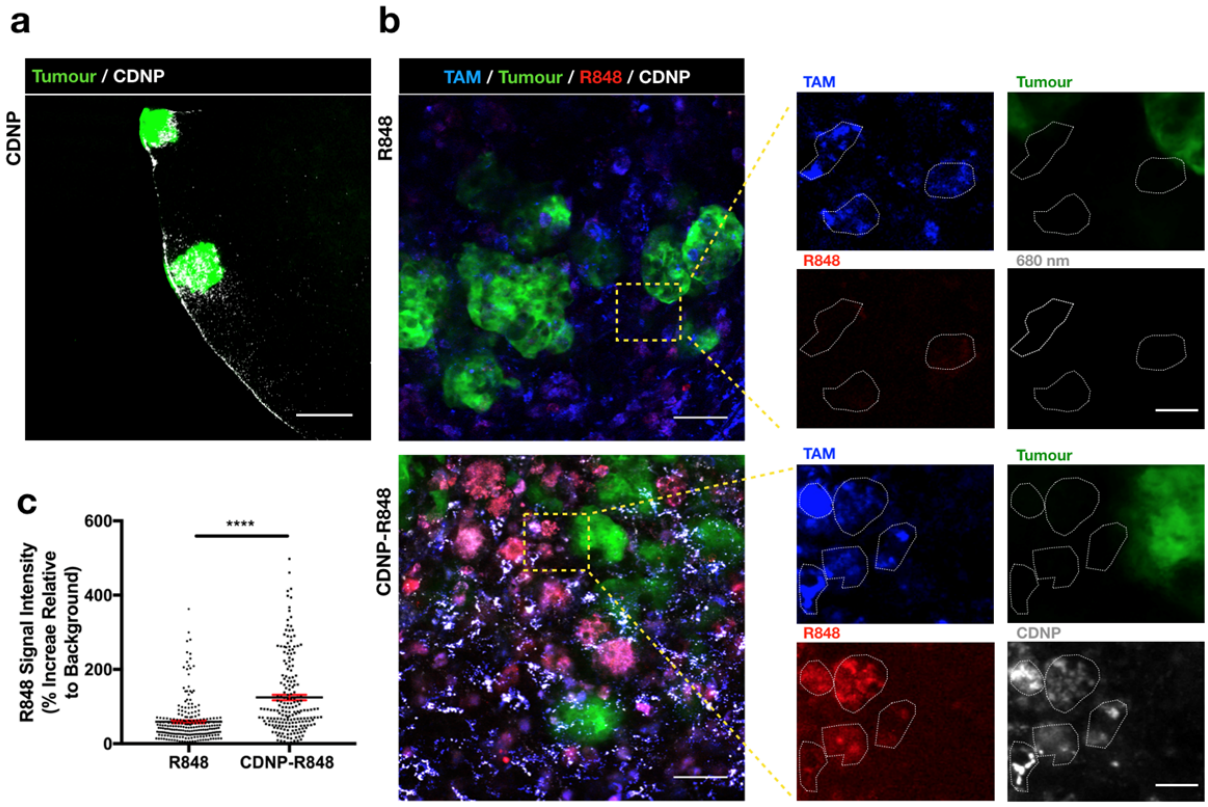

Supplementary Figure S10. CDNPs deliver R848 to tumour associated macrophage. Distribution of fluorescent analogues R848-BODIPY TMR X (red) and CDNP-VT680 (gray) was explored in C57BL/6 mice bearing eGFP expressing $Kras^{G12D}$ $p53^{-/-}$ mutant (KP) lung adenocarcinoma (tumour cells, green; [Ventura et al., 2007, #36341]). At 24 hours after injection (R848-BODIPY TMR + CD-succinate as a solublizer or R848-BODIPY TMR + CDNP-VT680), the lung lesions were imaged via confocal fluoresce microscopy to assess the distribution of R848 and CDNP, relative to dextran (blue) labelled macrophages in the tumours. All images are representative of observations across N=3 tumours per condition, each in a single mouse. **a**, Confocal fluorescent microscopy images showing CDNPs accumulate in the tumour lesions. **b**, High resolution fluorescent micrographs showing R848 and CDNP-VT680 distribution within the lung tumour lesions of mice treated with R848 (top) or CDNP-R848 (bottom). Notably, for mice treated with CDNP-R848, a strong co-localization of CDNP and R848 was observed within the TAMs, and CDNPs enhance the uptake of R848 by macrophages (bottom) compared to the R848 delivery alone (top). High magnification images (expanded) demonstrate co-localization of R848 and CDNP within TAMs, outlined (white) for clarity. **c**, Quantification of R848 signal intensity in TAMs; CDNP delivery enhanced the uptake of R848 by macrophages in the tumour microenvironment. Data represent mean ± s.e.m.; N = 228 cells (R848) and 198 cells (CDNP-R848); ****P<0.0001 (two-sided t-test). Scale bars: a, 1.0 mm; b, 50 μm; c, 10 μm.

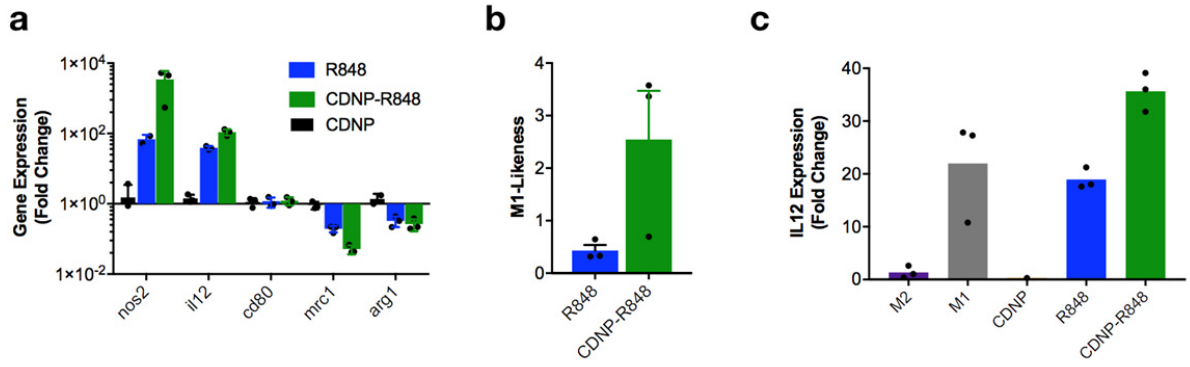

Supplementary Figure S11. Nanoparticle-assisted delivery of R848 enhances M1 re-education in murine and human macrophages *in vitro*. To examine macrophage re-education, both murine and human macrophages were polarized to an M2-state (IL-4 induction, 24 hrs) prior to drug treatment in the absence of IFN-γ. For all experiments, dosing was matched (100 nM R848, 24 hr). **a**, qPCR assessment of transcription expressed as fold change relative to M2 (IL-4 treated) controls. Data represent mean ± s.d., N=3 independent samples from a single experiment. CDNP-R848 treatment of murine macrophages enhances expression of M1-related genes (*nos2*, *il12b*, *cd80*) and further suppresses M2-related genes (*mrc1*, *arg1*), relative to treatment by R848 alone. Notably, the nanoparticle alone did not alter gene expression. **b,** M1-likeness is enhanced 5.9 fold following treatment by CDNP-R848 compared to R848 alone. Mean ± s.e.m.; N=3 independent samples from a single experiment; P=0.08 (two sided t-test). **c,** Expression of *il12b* by human macrophages treated by CDNP, R848, or CDNP-R848. M2-like and M1-like (LPS/INFγ treated) are provided for reference of baseline expression. Data represent mean fold change relative to *β-actin*, N=3 technical repeats from a single experiment.

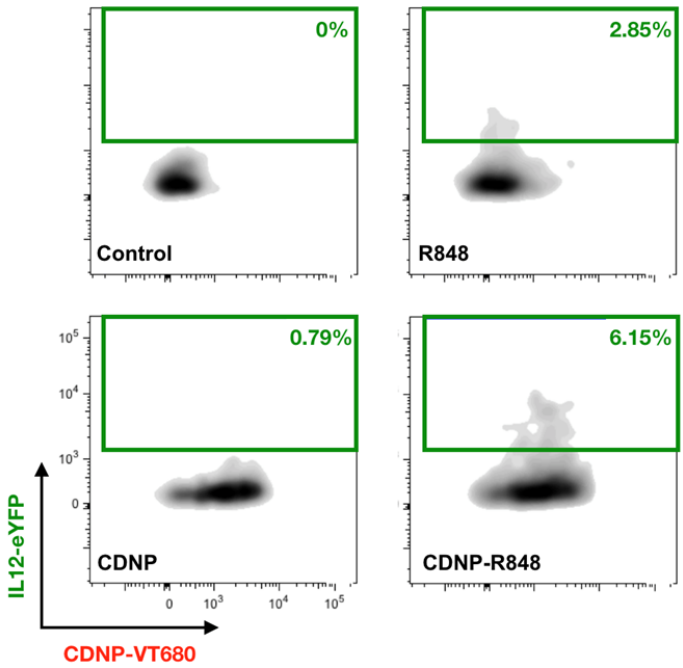

Supplementary Figure S12. Flow cytometry of TAM IL12 expression. Flow cytometry plots of tumour associated macrophages (CD45+, F4/80+) obtained from IL12-eYFP mice bearing wild type intradermal MC38 tumours at 24 hours following i.v. administration of saline (control), R848, CDNP, or CDNP-R848 each in a single mouse. For CDNP-R848 treatments (bottom right), indicated regions of high CDNP-VT680 signal and high IL12 expression (gated, green) demonstrating CDNP-R848 uptake is associated with highly elevated IL12 production.

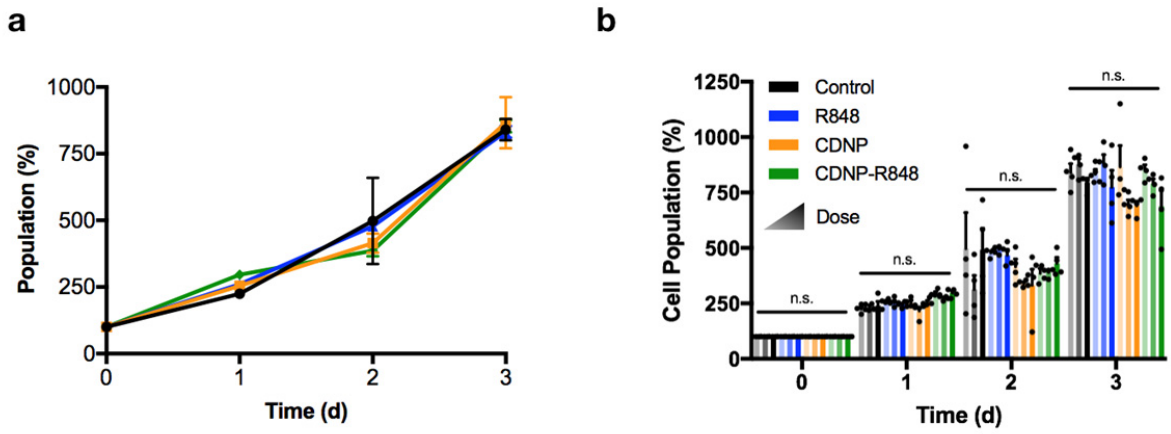

Supplementary Figure S13. Effect of R848 and nanoparticle formulation on cancer cell growth. MC38 cell proliferation was monitored (PrestoBlue assay) *in vitro* in the presence of vehicle (DMSO) control, R848, CDNP or matched dose of CDNP-R848. Data represent mean ± s.e.m. following normalization to baseline for each condition, N=4 independent samples per condition from a single experiment. **a,** Growth curves (10 nM R848) showed no effect on proliferation between groups. **b,** There was no change between groups at increased dose (10 nM, 100 nM, and 1.0 μM R848); two-way repeated measures ANOVA (group comparison P=0.103, Tukeys HSD (P>0.10)). Proliferation rate, determined by linear fit to each condition and dose, was unaltered by treatment conditions (P>0.96, F-test). None of the compounds demonstrated change in MC38 growth rate, indicating a lack of direct anticancer effects.

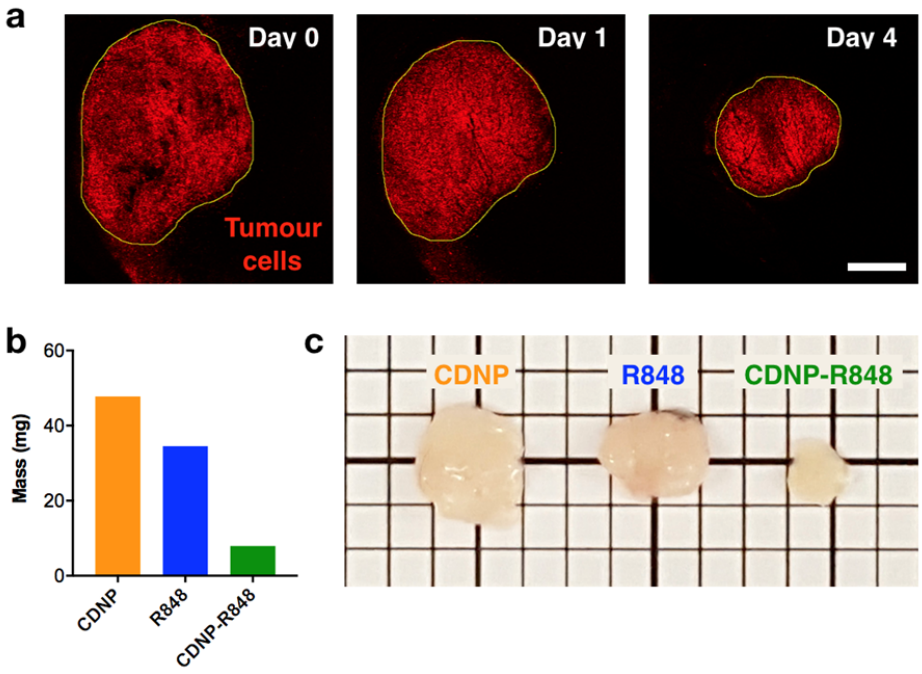

Supplementary Figure S14. Tumour regression following single-dose administration of CDNP-VT680. Tumour size was monitored following single-dose administration in IL12-eYFP mice on day 0 (8 days following tumour inoculation). **a,** Treatment with single-dose CDNP-R848 (16.5 mg kg^{-1} CDNP with 2.0 mg kg^{-1} R848) resulted in rapid tumour regression, observed by confocal fluorescence microscopy of a single, representative MC38–H2B-mApple tumour bearing mouse, outlined (yellow). Scale bar: 1.0 mm. **b-c,** Relative tumour sizes were determined by tumour weight (**b**) and gross imaging (**c**) of resected tumour tissues seven days after administration of R848 (2.0 mg kg^{-1}), CDNP (16.5 mg kg^{-1}), or CDNP (16.5 mg kg^{-1}) with R848 (2.0 mg kg^{-1}), each in a single MC38–H2B-mApple tumour bearing mouse. Drug nanoformulation resulted in smaller tumour size relative to CDNP and free drug controls, indicating feasibility of single-dose administration. Grids: 2.25 x 2.25 mm.

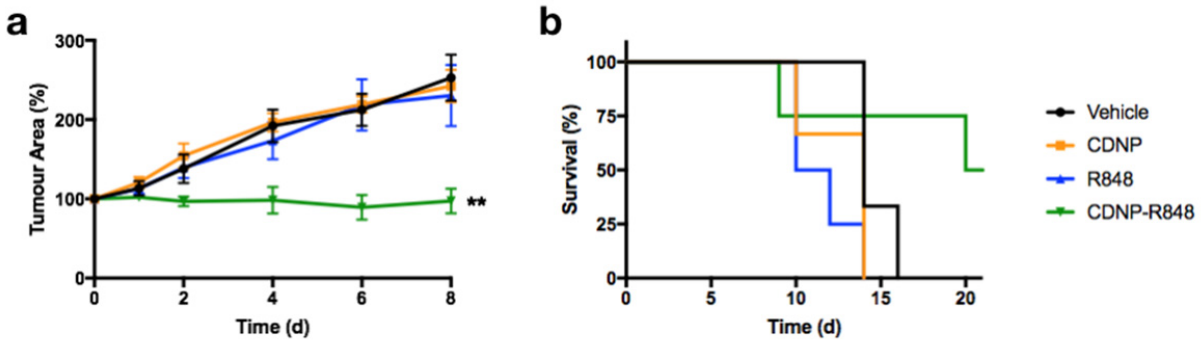

Supplementary Figure S15. Therapeutic efficacy of single dosing regimen. a, Tumour growth curves following treatment in C57BL/6 mice. Data are expressed as mean ± s.e.m; N=7 tumours per R848 and CDNP-R848 treatment group, N=6 tumours per vehicle and CDNP control group; **P=0.008 (Friedman, Dunn's multiple comparison) relative to vehicle control. **b,** Survival following start of treatment. N=4 mice per R848 and CDNP-R848 treatment group, N=3 mice per vehicle and CDNP control group. Treatments were initiated when tumours reached an area of 25 mm^2 (approximately 100mm^3).

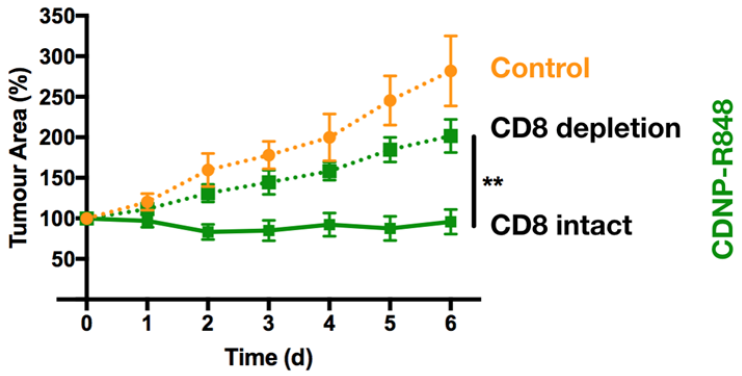

Supplementary Figure S16. Therapeutic efficacy of CDNP-R848 involved adaptive immunity. To examine the role of adaptive immune involvement, antibody depletion of CD8+ T-cells was examined in treatment groups, relative to CDNP controls in C57BL/6 mice bearing MC38 tumours. Growth curves following the start of treatment without or with depletion of CD8+ T-cells, following a single dose of CDNP (control) or CDNP-R848. Data are expressed as mean ± s.e.m; N=8 tumours per treatment group, N=7 tumours for control; **P=0.004 (Friedman, Dunn's multiple comparison) relative to CDNP control. All studies were executed in C57BL/6 mice, and treatment was initiated when tumours reached an area of 25 mm^2 (approximately 100 mm^3). Of note, CDNP-R848 treatment in the absence of CD8+ T-cells results in blunting but not complete elimination of treatment efficacy. All studies were performed in C57BL/6 mice, and treatment was initiated when tumours reached an area of 25 mm^2 (approximately 100mm^3).

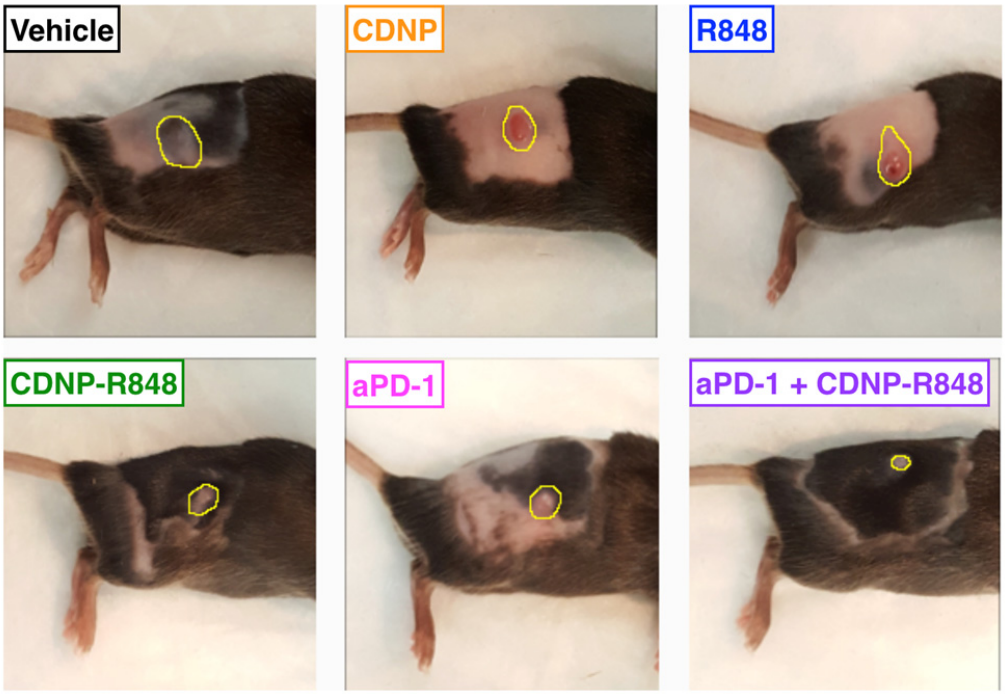

Supplementary Figure S17. Observed tumour growth in combination therapy. Images were acquired 7 days following administration of single agent (CDNP, CDNP-R848, aPD-1) or combination (aPD-1 + CDNP-R848) therapy in C57Bl/6 mice bearing MC38 tumours. Tumour margins are outlined (yellow). Images are representative of N=7 tumours per treatment group.

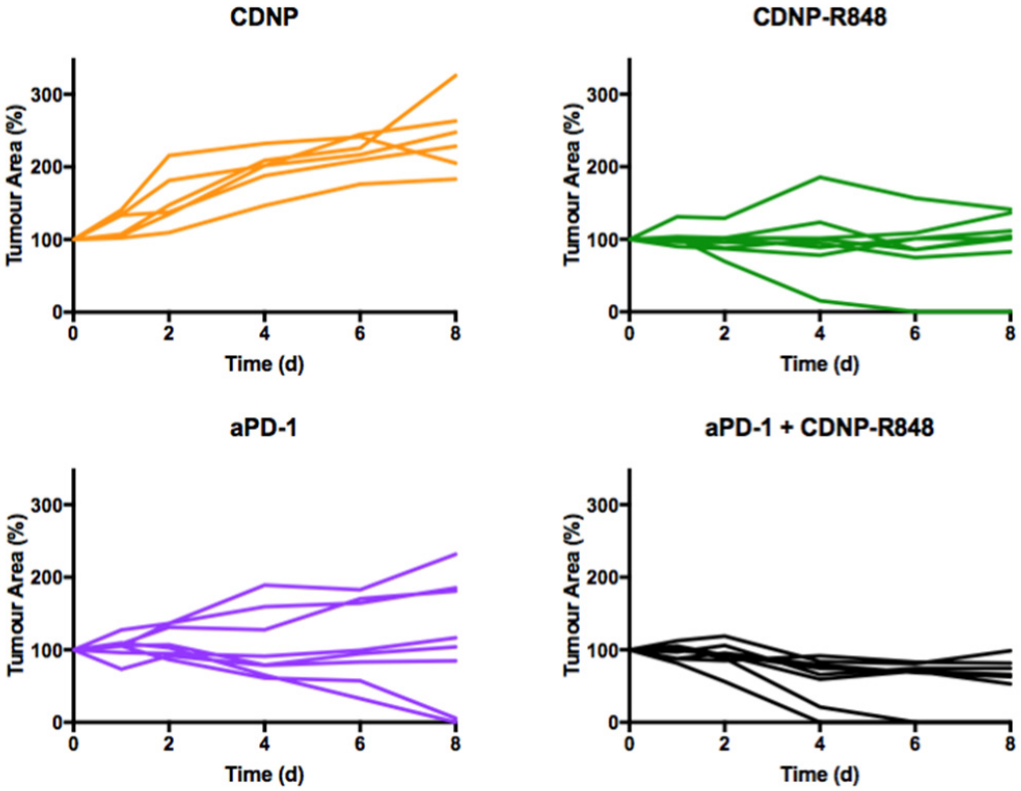

Supplementary Figure S18. Impact of combination therapy on treatment efficacy. Individual MC38 tumour growth curves in response to single agent (CDNP, CDNP-R848, aPD-1) or combination (aPD-1 + CDNP-R848) therapy in C57BL/6 mice bearing MC38 tumours. Heterogeneity of aPD-1 response is reduced by combination with CDNP-R848, and results in remarkably rapid tumour regression in some cases.

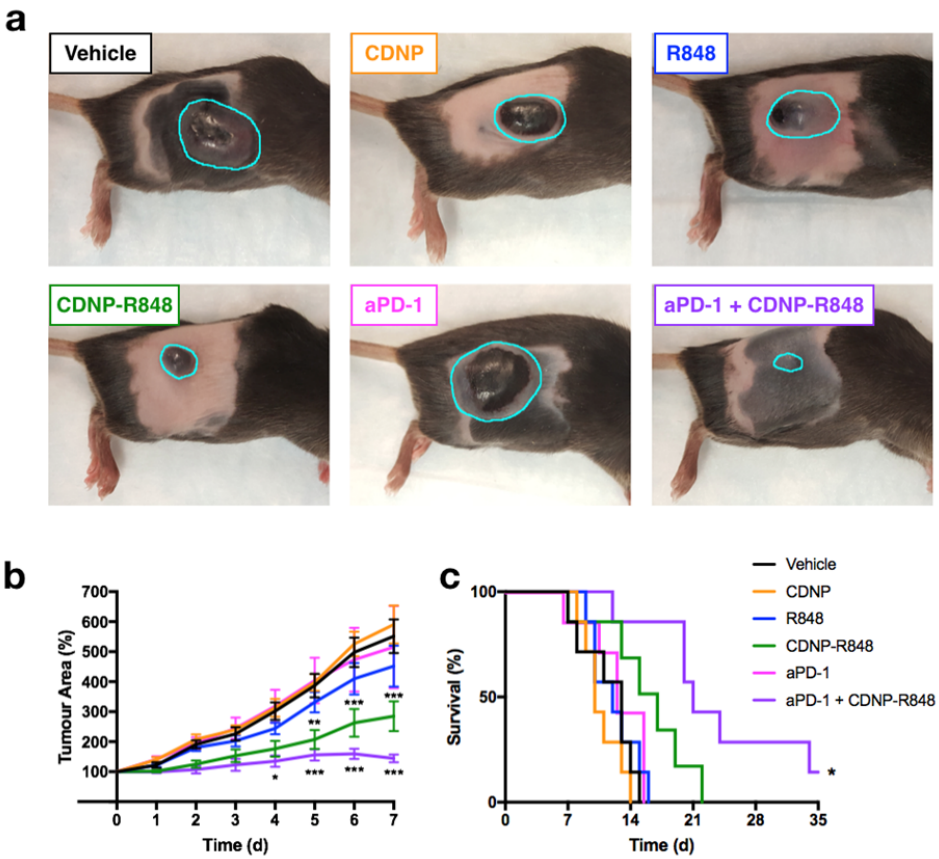

Supplementary Figure S19. Therapeutic efficacy of single administration and combination therapies against B16 melanoma. C57BL/6 mice bearing B16.F10 melanoma tumours were treated at day 8-9 following tumour inoculation, when tumours reached an established size (area of 25mm^2). Treatment was initiated by single dose administration of single agent (CDNP, CDNP-R848, aPD-1) or combination (aPD-1 + CDNP-R848) therapy. **a**, Macroscopic images of tumours at day 6 following initiation of treatment. Tumour margins are outlined (cyan) for clarity. **b**, Tumour growth curves following treatment. Data are expressed as mean ± s.e.m.; *P<0.05, **P<0.01, ***P<0.001 relative to vehicle controls (Dunnett multiple comparison). **c**, Survival (right) following start of treatment. *P=0.002 (Log-rank test, two-sided) relative to vehicle controls; N=7 animals.

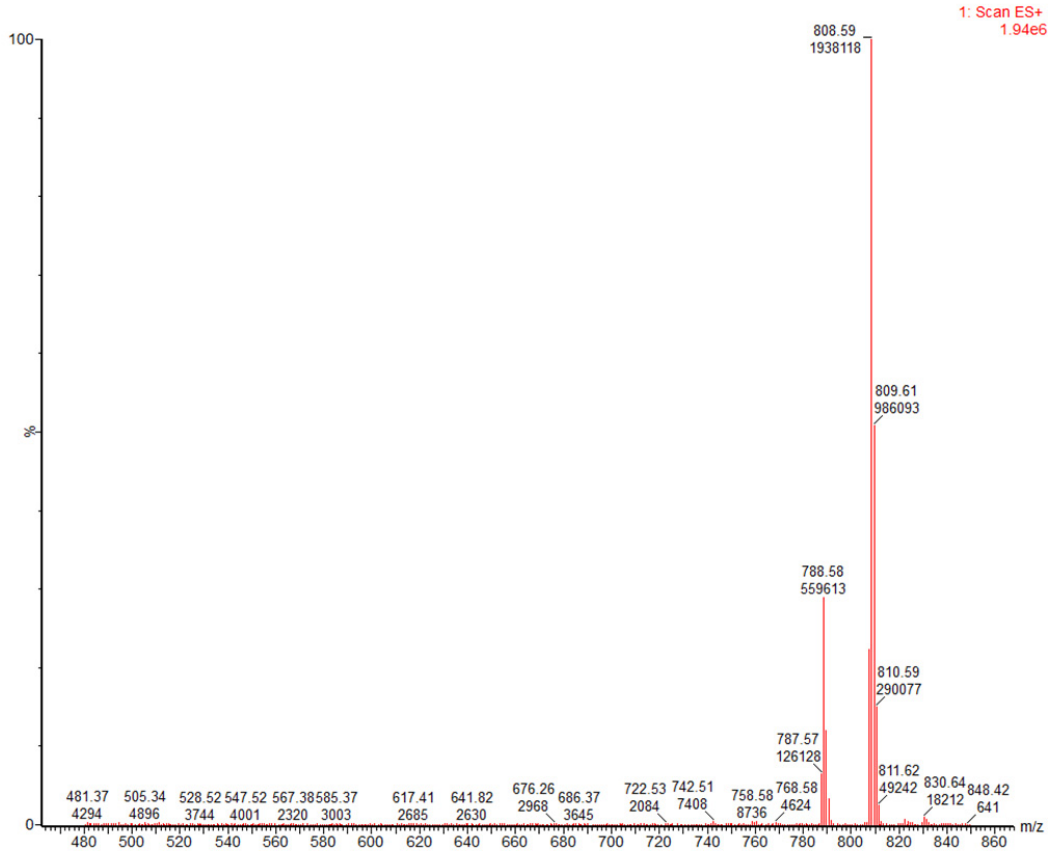

Supplementary Figure S20. Mass Spectroscopy Scan of R848-BODIPY TMR-X.

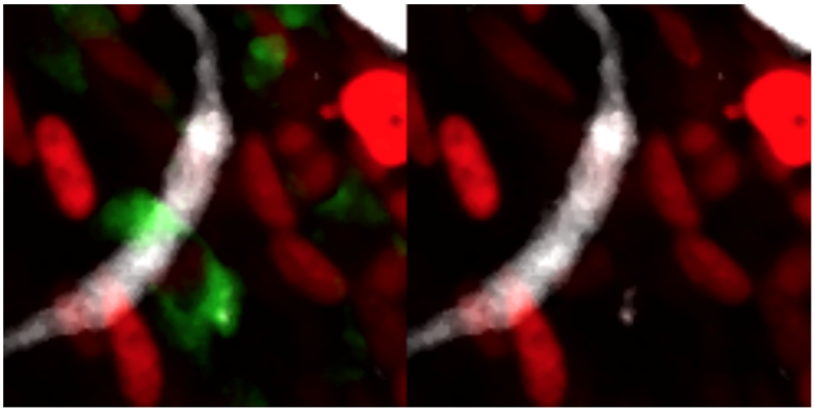

Movie S1. Rapid uptake of CDNPs by tumour associated macrophages *in vivo*. Intravital microscopy imaging of CDNP-VT680 injection in a NOD MerTK$^{GFP/+}$ mouse bearing a MC38–H2B-mApple tumour in a dorsal skinfold chamber. Time-lapse imaging was used to examine the distribution of CDNP-VT680. Following i.v. injection of CDNP-VT680 (0.5mg in 50µL saline) immediately prior to imaging, the nanoparticle can be observed in the vasculature with subsequent extravasation and accumulation in tumour associated macrophages (this is observed in all macrophages, but only one cell is highlighted here for clarity). To allow visualization of CDNP-VT680 within the macrophages, the GFP channel is not displayed in the right panel. These images are representative of N=3 independent experiments and are presented as projections of Z-stacks with 5 µm thickness, acquired over a total time course of 90 minutes. Scale bar: 25 µm.
Color scheme: CDNP-VT680 (white, nanoparticle), MC38-H2B-mApple (red, tumour cells), MerTK$^{GFP/+}$ (green, macrophages)

Supplementary References

1. Keliher, E. J. et al. Polyglucose nanoparticles with renal elimination and macrophage avidity facilitate PET imaging in ischaemic heart disease. *Nature communications* **8**, 14064 (2017).